Acta Oceanol. Sin., 2020, Vol. 39, No. 9, P. 133–139
https://doi.org/10.1007/s13131-020-1653-6
http://www.hyxb.org.cn
E-mail: hyxbe@263.net

An improved least mean square/fourth direct adaptive equalizer for under-water acoustic communications in the Arctic

Yanan Tian[1, 2, 3], Xiao Han[1, 2, 3]*, Jingwei Yin[1, 2, 3], Hongxia Chen[4], Qingyu Liu[5]

[1] Acoustic Science and Technology Laboratory, Harbin Engineering University, Harbin 150001, China

[2] Key Laboratory of Marine Information Acquisition and Security (Harbin Engineering University), Ministry of Industry and Information Technology, Harbin 150001, China

[3] College of Underwater Acoustic Engineering, Harbin Engineering University, Harbin 150001, China

[4] First Institute of Oceanography, Ministry of Natural Resources, Qingdao 266061, China

[5] Naval Research Academy, Beijing 100161, China

Received 13 October 2019; accepted 13 November 2019

Abstract

An improved least mean square/fourth direct adaptive equalizer (LMS/F-DAE) is proposed in this paper for underwater acoustic communication in the Arctic. It is able to process complex-valued baseband signals and has better equalization performance than LMS. Considering the sparsity feature of equalizer tap coefficients, an adaptive norm (AN) is incorporated into the cost function which is utilized as a sparse regularization. The norm constraint changes adaptively according to the amplitude of each coefficient. For small-scale coefficients, the sparse constraint exists to accelerate the convergence speed. For large-scale coefficients, it disappears to ensure smaller equalization error. The performance of the proposed AN-LMS/F-DAE is verified by the experimental data from the 9th Chinese National Arctic Research Expedition. The results show that compared with the standard LMS/F-DAE, AN-LMS/F-DAE can promote the sparse level of the equalizer and achieve better performance.

Key words: underwater acoustic communication, the Arctic, direct adaptive equalizer, adaptive norm

Citation: Tian Yanan, Han Xiao, Yin Jingwei, Chen Hongxia, Liu Qingyu. 2020. An improved least mean square/fourth direct adaptive equalizer for under-water acoustic communications in the Arctic. Acta Oceanologica Sinica, 39(9): 133–139, doi: 10.1007/s13131-020-1653-6

1 Introduction

With the rapid development of various applications in the Arctic in recent years, more and more ocean observation equipment such as underwater unmanned vehicle (UUV) is being used in the Arctic to gain insight into the temporal and spatial processes below the ice surface (Wang et al., 2017; Li et al., 2019). However, the thick ice covered in the Arctic prevents underwater platforms from communicating with the satellites, which makes acoustics the only means of data transmissions under ice surface. Different from open-water environment, under-ice environment can introduce some new problems for acoustic communication such as larger transmission loss, severe Doppler effect, and impulsive noise. The key feature of the typical Arctic sound speed profile is that the minimum sound speed resides at the ice-water interface (Freitag et al., 2012). According to the ray theory, all of the acoustic energy in this typical Arctic environment will interact with the ice cover. Because of the roughness of the ice cover, acoustic interactions with the ice cause significant scattering and therefore significant losses. When communicating in the floating ice area, the acoustic rays which are reflected by time-varying rough ice surface can introduce random Doppler effect which makes it difficult to compensate the phase of received signals. There are also many ice cracking or ice collision activities in the Arctic, producing a lot of impulsive noise which makes it challenge work to achieve robust communication performance.

The inter-symbol interference (ISI) caused by multipath spread and the Doppler shift owing to the relative motion make the channel equalization at the receiving end a challenging task for underwater acoustic (UWA) communications (Berger et al., 2010; Liu et al., 2017). Two representative methods in channel equalization are frequency domain equalization (Falconer et al., 2002) and time domain equalization (Vanbleu et al., 2006). The former has a lower computational complexity, but it cannot track channel changes in time for the reason that it operates in block units. Two important classifications in time domain equalization are direct adaptive equalizer (DAE) which obtains the equalizer coefficients directly from the received data, and channel estimation based equalizer (CEBE) using the received signal to get the channel taps and then calculating the equalizer coefficients (Pelekanakis and Chitre, 2013). When the signal to noise ratio (SNR) is low, the performance of the two is similar, but the calculation complexity of DAE is low (Lee and Cox, 1997). The DAE with an embedded phase-locked loop (PLL) has been successfully applied in UWA channel equalization for many years (Sto-

Foundation item: The National Natural Science Foundation of China under contract Nos 61631008 and 61901136; the National Key Research and Development Program of China under contract No. 2018YFC1405904; the Fok Ying-Tong Education Foundation under contract No. 151007; the Heilongjiang Province Outstanding Youth Science Fund under contract No. JC2017017; the Opening Funding of Science and Technology on Sonar Laboratory under contract No. 6142109KF201802; the Innovation Special Zone of National Defense Science and Technology.

*Corresponding author, E-mail: hanxiao1322@hrbeu.edu.cn

janovic et al., 1993).

The UWA equalizer exhibits sparse features due to the sparsity of the UWA channel itself, which means that most coefficients are close to zero (Vlachos et al., 2012; Li and Preisig, 2007). Inspired by sparse adaptive filtering theory, attempts at combining sparse nature with adaptive equalizers have gained considerable interest. Pelekanakis and Chitre (2010) apply improved proportionate normalized least mean square (IPNLMS) to the decision feedback equalization (DFE). The results prove its superiority when sparse channel is encountered and it also shows robustness for non-sparse channel. Duan et al. (2018) use the IPNLMS to update the coefficients of the Turbo equalizer. It speeds up the convergence of large taps with good tracking ability and low computational complexity. Chen et al. (2009) add the norm penalties to the cost function and exploit them as sparse regularizations, thus obtaining zero-attracting LMS (ZA-LMS) and reweighted ZA-LMS (RZA-LMS), which gain additional performance. In Tao et al. (2017), authors propose selective ZA-NLMS (SZA-NLMS) equalization method. Compared with ZA-NLMS, it does not impose the same penalty on all coefficients uniformly, but limits the scope of constraints, further improving the performance of the equalizer. The LMS equalizer is widely used due to the simplicity of operation and small amount of calculation. However, it is sensitive to input signals and SNR, and the performance is severely degraded especially under low SNR (Guan et al., 2013b). Recursive least square (RLS) can overcome such problems, and methods employing RLS constrained by sparse features have also appeared. RLS penalized by a general convex function is proposed in (Eksioglu and Tanc, 2011). It can adaptively adjust the strength of the sparse constraint according to certain criteria, so the performance improves significantly. However, the computational complexity of RLS increases as the square of the length of the equalizer (Eksioglu, 2014). When the UWA channel multipath expansion is severe, the computational complexity is extremely high. The least mean fourth (LMF) based on high order moment is also an effective method to overcome noise (Walach and Widrow, 1984). It utilizes the fourth power instead of the square power of the equalization error. According to the theory in Mendel (1991), the high-order energy filter can suppress the noise interference better, and can overcome the shortcomings of the LMS. However, its computational complexity is still very high. Combining the advantages of LMS and LMF, the LMS/F algorithm can effectively improve the performance of LMS without sacrificing its simplicity and stability. The performance of LMS/F has proven to be better than that of traditional LMS and LMF (Guan et al., 2013b). Using the sparse nature of the channel, the ZA-LMS/F and RZA-LMS/F channel estimation algorithms constrained by the l_1 norm or the weighted l_1 norm have been proposed (Guan et al., 2013a). However, few papers mention the application of the sparse LMS/F algorithm to the equalizer. Moreover, the sparse LMS/F algorithm mentioned above is performed in the real domain, which is not suitable for processing baseband complex signals in UWA systems. In this paper, we propose a LMS/F-DAE algorithm with adaptive norm constrained. Compared with the traditional LMS/F algorithm, it has two improvements: (1) Extend the LMS/F only suitable for processing real signals to the complex domain to process the baseband UWA signals. (2) Adaptively assign sparse penalty terms to each equalizer coefficient to improve the sparse level and the equalization performance.

The rest of the paper is organized as follows: Section 2 specifically gives the derivation process of adaptive norm LMS/F-DAE (AN-LMS/F-DAE); in Section 3, we process the experimental data from the 9th Chinese National Arctic Research Expedition to verify its reliability and effectiveness; Section 4 summarizes the whole paper.

Note: the vector is shown in bold black. The superscripts "H" "T" and "*" indicate the Hermitian transpose, transpose, and conjugate operation respectively. For a complex value a, the sign function is defined as: $\mathrm{sign}(a)=\begin{cases}\dfrac{a}{2|a|}, & a\neq 0\\ 0, & a=0\end{cases}$, and for complex vector $\boldsymbol{x}$ of length N, the p norm is expressed as $||\boldsymbol{x}||_p^p=\sum_{i=1}^{N}|x_i|^p=\sum_{i=1}^{N}(x_i x_i^*)^{\frac{p}{2}}, 0\leqslant p\leqslant 2$. For vectors $\boldsymbol{x}=[x_1\ x_2\ x_3\ \cdots\ x_N]^{\mathrm{T}}$ and $\boldsymbol{y}=[y_1\ y_2\ y_3\ \cdots\ y_N]^{\mathrm{T}}$, the element-wise multiplication, division and power are defined as $\boldsymbol{z}_1=\boldsymbol{xy}=[x_1y_1\ x_2y_2\ x_3y_3\ \cdots\ x_Ny_N]^{\mathrm{T}}$, $\boldsymbol{z}_2=\dfrac{\boldsymbol{x}}{\boldsymbol{y}}=\left[\dfrac{x_1}{y_1}\ \dfrac{x_2}{y_2}\ \dfrac{x_3}{y_3}\ \cdots\ \dfrac{x_N}{y_N}\right]^{\mathrm{T}}$ and $\boldsymbol{z}_3=\boldsymbol{x}^{\boldsymbol{y}}=[x_1^{y_1}\ x_2^{y_2}\ x_3^{y_3}\ \cdots\ x_N^{y_N}]^{\mathrm{T}}$, respectively.

2 Proposed AN-LMS/F-DAE

The output of a DAE at instant n is $\hat{x}_n=\mathrm{e}^{-j\theta_n}\boldsymbol{w}_n^{\mathrm{H}}\boldsymbol{r}_n-\boldsymbol{f}_n^{\mathrm{H}}\tilde{\boldsymbol{x}}_n$, where θ_n compensates for the effects of phase deflection whose size is controlled by a second-order PLL; $\boldsymbol{w}_n=[w_{n,0}\ w_{n,1}\ w_{n,2}\cdots\ w_{n,K}]^{\mathrm{T}}$ is the feed-forward filter coefficient vector with $K+1$ length at instant n; $\boldsymbol{r}_n=[r_{n+K}\ r_{n+K-1}\ r_{n+K-2}\ \cdots\ r_n\ ]^{\mathrm{T}}$ is a sequence of received symbols; $\boldsymbol{f}_n=[f_{n,0}\ f_{n,1}\ f_{n,2}\ \cdots\ f_{n,L}]^{\mathrm{T}}$ is the feedback filter coefficient vector with $L+1$ length; $\tilde{\boldsymbol{x}}_n=[\tilde{x}_{n-1}\ \tilde{x}_{n-2}\ \tilde{x}_{n-3}\ \cdots\ \tilde{x}_{n-L-1}]^{\mathrm{T}}$ is the symbol vector which has been decided before n. If $\boldsymbol{f}_n^{\mathrm{H}}\tilde{\boldsymbol{x}}_n$ disappears, it is a linear DAE. Otherwise, it is a DFE. The equalization error can be expressed as $e_n=x_n-\hat{x}_n=x_n-\mathrm{e}^{-j\theta_n}\boldsymbol{w}_n^{\mathrm{H}}\boldsymbol{r}_n+\boldsymbol{f}_n^{\mathrm{H}}\tilde{\boldsymbol{x}}_n$, where x_n is the desired signal. Inspiring by standard LMS/F cost function (Guan et al., 2013b) and taking the sparse feature into consideration, the cost function of LMS/F-DAE penalized by norm constraint is defined as:

$$J_n=e_n^2-\varepsilon\ln(e_n^2+\varepsilon)+\gamma_w||\boldsymbol{w}_n||_p^p+\gamma_f||\boldsymbol{f}_n||_p^p. \tag{1}$$

The first two terms in Eq. (1) are the same as those in standard LMS/F, where $\varepsilon>0$ is a threshold that compromises between convergence speed and equalization error; and the last two terms are sparse norm constraints with $\gamma_w,\gamma_f\geqslant 0$ measuring the strength. Using the complex domain gradient descent recursion method (Brandwood, 1983), the update process is:

$$\begin{cases}\boldsymbol{w}_{n+1}=\boldsymbol{w}_n-\mu_w\dfrac{\partial J_n}{\partial\boldsymbol{w}_n^*}\\ \boldsymbol{f}_{n+1}=\boldsymbol{f}_n-\mu_f\dfrac{\partial J_n}{\partial\boldsymbol{f}_n^*}\end{cases}, \tag{2}$$

where μ_w and μ_f are the step sizes which affect the convergence speed and steady state error. $\dfrac{\partial J_n}{\partial\boldsymbol{w}_n^*}$ and $\dfrac{\partial J_n}{\partial\boldsymbol{f}_n^*}$ represent the direction in which the cost function J_n changes the fastest along $\boldsymbol{w}_n$ and $\boldsymbol{f}_n$, respectively. Taking Eq. (1) into Eq. (2), we get:

$$\begin{aligned}\frac{\partial J_n}{\partial\boldsymbol{w}_n^*}&=\frac{\partial(e_n^2-\varepsilon\ln(e_n^2+\varepsilon))}{\partial\boldsymbol{w}_n^*}+\gamma_w\frac{\partial||\boldsymbol{w}_n||_p^p}{\partial\boldsymbol{w}_n^*}\\&=e_n^*\frac{\partial e_n}{\partial\boldsymbol{w}_n^*}-\varepsilon\frac{e_n^*}{e_n^2+\varepsilon}\frac{\partial e_n}{\partial\boldsymbol{w}_n^*}+\gamma_w\frac{p}{2}(\boldsymbol{w}_n\boldsymbol{w}_n^*)^{\frac{p}{2}-1}\boldsymbol{w}_n\\&=(e_n^*-\varepsilon\frac{e_n^*}{e_n^2+\varepsilon})\frac{\partial e_n}{\partial\boldsymbol{w}_n^*}+\frac{\gamma_w p}{2}\frac{\boldsymbol{w}_n}{|\boldsymbol{w}_n|^{2-p}}\\&=-\frac{e_n^*e_n^2}{e_n^2+\varepsilon}e^{-j\theta}\boldsymbol{r}_n+\frac{\gamma_w p}{2}\frac{\boldsymbol{w}_n}{|\boldsymbol{w}_n|^{2-p}}.\end{aligned} \tag{3}$$

Note that $\boldsymbol{w}_n\boldsymbol{w}_n^*$ and $\frac{\boldsymbol{w}_n}{|\boldsymbol{w}_n|^{2-p}}$ are element-wise multiplication and division, respectively. The same procedure can be easily adapted to $\frac{\partial J_n}{\partial \boldsymbol{f}_n^*}$ and the result is:

$$\begin{aligned}\frac{\partial J_n}{\partial \boldsymbol{f}_n^*} &= \frac{\partial(e_n^2 - \varepsilon\ln(e_n^2+\varepsilon))}{\partial \boldsymbol{f}_n^*} + \gamma_f\frac{\partial\|\boldsymbol{f}_n\|_p^p}{\partial \boldsymbol{f}_n^*}\\ &= \frac{e_n^* e_n^2}{e_n^2+\varepsilon}\tilde{\boldsymbol{x}}_n + \frac{\gamma_f p}{2}\frac{\boldsymbol{f}_n}{|\boldsymbol{f}_n|^{2-p}}.\end{aligned} \tag{4}$$

Bring Eqs (3) and (4) into Eq. (2) to get the update equation as:

$$\boldsymbol{w}_{n+1} = \boldsymbol{w}_n + \mu_w\frac{e_n^* e_n^2}{e_n^2+\varepsilon}\mathrm{e}^{-j\theta}\boldsymbol{r}_n - \frac{\mu_w\gamma_w p}{2}\frac{\boldsymbol{w}_n}{|\boldsymbol{w}_n|^{2-p}}, \tag{5}$$

$$\boldsymbol{f}_{n+1} = \boldsymbol{f}_n - \mu_f\frac{e_n^* e_n^2}{e_n^2+\varepsilon}\tilde{\boldsymbol{x}}_n - \frac{\mu_f\gamma_f p}{2}\frac{\boldsymbol{f}_n}{|\boldsymbol{f}_n|^{2-p}}. \tag{6}$$

The first two terms of Eqs (5) and (6) are the LMS/F update formulas when no sparse constraints are applied. It can be seen that when $\varepsilon \ll e_n^2$, they behave like LMS with step sizes μ_w and μ_f; when $\varepsilon \gg e_n^2$, they show the same performance as LMF with step sizes μ_w/ε and μ_f/ε. The last items in Eqs (5) and (6) are ZA terms characterizing the sparse feature. It gains considerable performance by speeding up the convergence of the near-zero coefficients. It should also be noted that, like l_0-LMS and l_1-LMS, the presence of the last term introduces additional errors while improving the sparse level. The parameter p is adjustable which has an influence on both the sparse level and the equalization performance. If different values p are assigned to different taps, the sparse level and the equalization error performance may be improved at the same time. Rewriting Eqs (5) and (6) as:

$$\begin{cases}\boldsymbol{w}_{n+1} = \boldsymbol{w}_n + \mu_w\dfrac{e_n^* e_n^2}{e_n^2+\varepsilon}\mathrm{e}^{-j\theta}\boldsymbol{r}_n - \dfrac{\mu_w\gamma_w\boldsymbol{p}_w}{2}\dfrac{\boldsymbol{w}_n}{|\boldsymbol{w}_n|^{2-\boldsymbol{p}_w}}\\ \boldsymbol{p}_w = [p_{w,0}\ p_{w,1}\ p_{w,2}\cdots p_{w,K}]\end{cases}, \tag{7}$$

$$\begin{cases}\boldsymbol{f}_{n+1} = \boldsymbol{f}_n - \mu_f\dfrac{e_n^* e_n^2}{e_n^2+\varepsilon}\tilde{\boldsymbol{x}}_n - \dfrac{\mu_f\gamma_f\boldsymbol{p}_f}{2}\dfrac{\boldsymbol{f}_n}{|\boldsymbol{f}_n|^{2-\boldsymbol{p}_f}}\\ \boldsymbol{p}_f = [p_{f,0}\ p_{f,1}\ p_{f,2}\ \cdots\ p_{f,L}]\end{cases}. \tag{8}$$

Note that $|\boldsymbol{w}_n|^{2-\boldsymbol{p}_w}$ and $|\boldsymbol{f}_n|^{2-\boldsymbol{p}_f}$ are element-wise powers. Equations (7) and (8) demonstrate that by introducing vectors $\boldsymbol{p}_w$ and $\boldsymbol{p}_f$, different p values are distributed to different taps to change the strength of sparse constraint. For the small equalizer coefficients, we want to enhance the sparse constraint to improve the sparse level; while for large coefficients, we hope the constraint to be weak or non-existent to reduce the equalization error.

Considering the form of Eqs (7) and (8) and inspired by (Wu and Tong, 2013), the mean value of the tap coefficients is introduced as the criterion for measuring the coefficient "large" or "small". At instant n, taking the expectations of feed-forward and feed-back taps as a division metric:

$$\begin{cases}m_{w,n} = E(|\boldsymbol{w}_{n-1}|)\\ m_{f,n} = E(|\boldsymbol{f}_{n-1}|)\end{cases}. \tag{9}$$

When a coefficient is less than $m_{w,n}$ or $m_{f,n}$, classify it as the "small" type. p should be selected to avoid too weak or too strong sparse constraints due to different sizes of $w_{n,i}$ or $f_{n,i}$. At this time, we choose $p = 1$ to speed up the convergence while reducing computational complexity. When a coefficient is greater than $m_{w,n}$ or $m_{f,n}$, classify it as the "large" type. In order to reduce the equalization error, we do not impose sparse constraints on it. The criterion of selecting p is:

$$\begin{cases}\arg\min\limits_{p_{w,i}}\left[\dfrac{p_{w,i}}{|w_{n,i}|^{2-p_{w,i}}}\right] = 0\\ \arg\min\limits_{p_{f,i}}\left[\dfrac{p_{f,i}}{|f_{n,i}|^{2-p_{f,i}}}\right] = 0\end{cases}, \tag{10}$$

where $p_{w,i}, p_{f,i}$ are the i-th element of $\boldsymbol{p}_w$ and $\boldsymbol{p}_f$, $w_{n,i}$ and $f_{n,i}$ denote the i-th element of $\boldsymbol{w}_n$ and $\boldsymbol{f}_n$, respectively. Then we choose $p_i = 0$ under this condition. Based on the above analysis, the update equation becomes:

$$w_{n+1,i} = \begin{cases}w_{n,i} + \mu_w\dfrac{e_n^* e_n^2}{e_n^2+\varepsilon}\mathrm{e}^{-j\theta}r_{n,i} - \mu_w\gamma_w\mathrm{sign}(w_{n,i}),\ \text{if } |w_{n,i}| \leqslant m_{w,n}\\ w_{n,i} + \mu_w\dfrac{e_n^* e_n^2}{e_n^2+\varepsilon}\mathrm{e}^{-j\theta}r_{n,i}, \qquad \text{else}\end{cases} \quad 0 \leqslant i \leqslant K, \tag{11}$$

$$f_{n+1,i} = \begin{cases}f_{n,i} - \mu_f\dfrac{e_n^* e_n^2}{e_n^2+\varepsilon}\tilde{x}_{n,i} - \mu_f\gamma_f\mathrm{sign}(f_{n,i}),\ \text{if } |f_{n,i}| \leqslant m_{f,n}\\ f_{n,i} - \mu_f\dfrac{e_n^* e_n^2}{e_n^2+\varepsilon}\tilde{x}_{n,i}, \qquad \text{else}\end{cases} \quad 0 \leqslant i \leqslant L, \tag{12}$$

where $r_{n,i}$, $\tilde{x}_{n,i}$ represent the i-th element of $\boldsymbol{r}_n$ and $\tilde{\boldsymbol{x}}_n$, respectively. Equations (11) and (12) indicate that AN-LMS/F-DAE imposes different sparse constraints on different coefficients: it exerts l_1-norm constraint on small coefficients while exerting no constraints on large ones. Therefore, it can compromise between sparse level and steady-state error to improve equalizer performance.

3 Experimental results in the Arctic

During the 9th Chinese National Arctic Research Expedition, underwater acoustic communication experiments are conducted between short-term ice stations and the R/V *Xuelong* at range 500 m and 4 km. The schematic diagram of underwater acoustic communication experiments is shown in Fig. 1, where a vertical receiving array with five self-recording hydrophones is deployed from short-term ice stations and a transducer with a frequency band of 2–8 kHz is deployed from the middle deck of R/V *Xuelong*. The hydrophones in the vertical receiving array are uniformly spaced by 10 m and the top element is deployed to 20 m depth. The transducer is deployed to 50 m depth. The superiority of the proposed AN-LMS/F-DAE will be verified using data from these experiments.

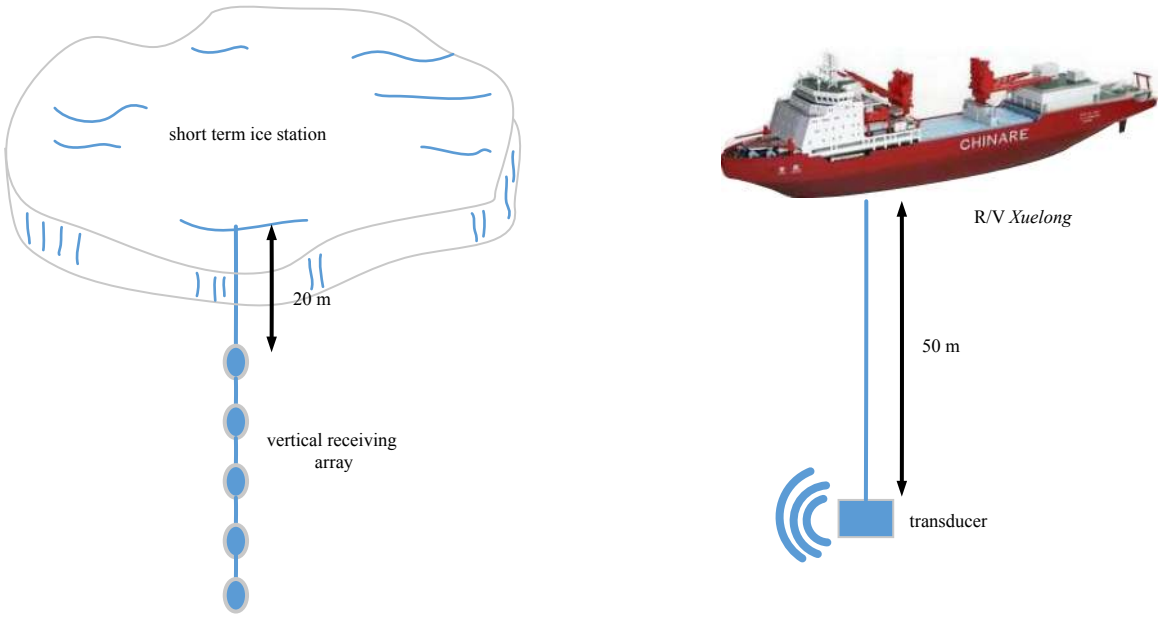

Fig. 1. The schematic diagram of underwater acoustic communication experiment.

The communication sequences are modulated by BPSK and QPSK, the transmitted waveform is pulse shaped using a raised-cosine filter with a roll-off factor 1. The center frequency is 3 kHz and the used frequency band is 2–4 kHz, the symbol rate is 1 ksymbols/s, the communication rates corresponding to BPSK and QPSK modulated signal are 1 kbps and 2 kbps respectively, and all signals are sampled at 48 kHz. A total of 11 000 bits data are transmitted for BPSK modulated signal while 22 000 bits data for QPSK modulated signal.

To demonstrate the superiority of the proposed algorithm, we choose another sparse equalizer called selective zero-attracting LMS (SZA-LMS) (Tao et al., 2017) as a comparison. In DAE, accurate channel structure is not necessary. However, channel length is needed as it is related to the choice of equalizer parameter K and L. According to the estimated channels in our experiments, the maximum channel delay is about 20 ms, corresponding to 20 symbols. Based on this priori information, we set the tap length of feed-forward filter as $K=30$ (slightly bigger than the maximum channel delay) and the tap length of feedback filter as $L=30$ (also slightly bigger than the maximum channel delay), which provide a clear comparison between different equalization methods. Though such a choice of K and L is sub-optimal considering complexity performance. The parameters of the second order PLL are $PLL_1=0.000\ 1,\ PLL_2=PLL_1/10$.

3.1 *Experimental results at range 500 m*

Figure 2 shows the channel impulse responses (CIRs) at different depths at range 500 m. Note that the self-recording hydrophone at 20 m could not work normally, so it is excluded when processing experimental data. It can be seen from Fig. 2 that (1) the channels show sparse feature and there are one or two distinct paths at different depths; (2) the channels are very stable throughout the whole signal duration with a small multipath spread (<10 ms); and (3) the first arrived path does not necessarily have the strongest power as shown in Fig. 2b.

For experimental data at range 500 m, the SNR is relatively high because the distance is very close. In order to show the superior performance of the proposed algorithm at low SNR, additional ambient noise is superimposed to the received signal to reduce the SNR around 6.1 dB. The step size is set to be 0.001. Other parameters are to adjusted constantly and chosen the corresponding values when the bit error rate (BER) performance is optimal. In AN-LMS/F-DAE, we choose $\gamma_w=3e-1, \gamma_f=8e-3, \varepsilon=2$ for BPSK signal and $\gamma_w=4e-2, \gamma_f=1e-3, \varepsilon=2$ for QPSK signal; in SZA-LMS-DAE, $\beta=0.5, \gamma_1=3e-1, \gamma_2=8e-3$ for BPSK signal and $\beta=0.5, \gamma_1=4e-2, \gamma_2=1e-3$ for QPSK signal. The amplitude comparison of the equalizer coefficients obtained by LMS/F-DAE and AN-LMS/F-DAE is shown in Fig. 3 which illustrates that large-scale coefficients only account for a small part of the whole range elements. It can be observed that the coefficients obtained by AN-LMS/F-DAE are sparser compared with that obtained by LMS/F-DAE. This is because we apply extra penalty terms to improve the sparse property, thus the small coefficient keeping close to zero during the convergence process.

Then we compare the BER performance of LMS-DAE, SZA-LMS-DAE, LMS/F-DAE and AN-LMS/F-DAE under different training sequence lengths (TSLs) when BPSK or QPSK modulated signal is presented. It can be seen from the results shown in Fig. 4 that (1) the LMS/F-DAE has a lower BER and a better equalization performance compared with LMS-DAE; (2) when applying sparse constraints to LMS-DAE and LMS/F-DAE, the resulting SZA-LMS-DAE and AN-LM/S-DAE have better performance compared with their corresponding standard methods; and (3) AN-LMS/F-DAE has the fastest convergence speed as expected, and the equalization error of AN-LMS/F-DAE is comparable or slightly better than that of LMS/F-DAE. The reason can be explained as follows: AN-LMS/F-DAE imposes constraints on small coefficients to make them converge quickly, and does not impose constraints on large ones to ensure correct convergence to reduce equalization error, so it can achieve good performance in terms of convergence speed and BER performance.

3.2 *Experimental results at range 4 km*

Figure 5 shows the CIRs at different depths at range 4 km. Note that the self-recording hydrophone at 40 m could not work normally, so it is excluded when processing experimental data.

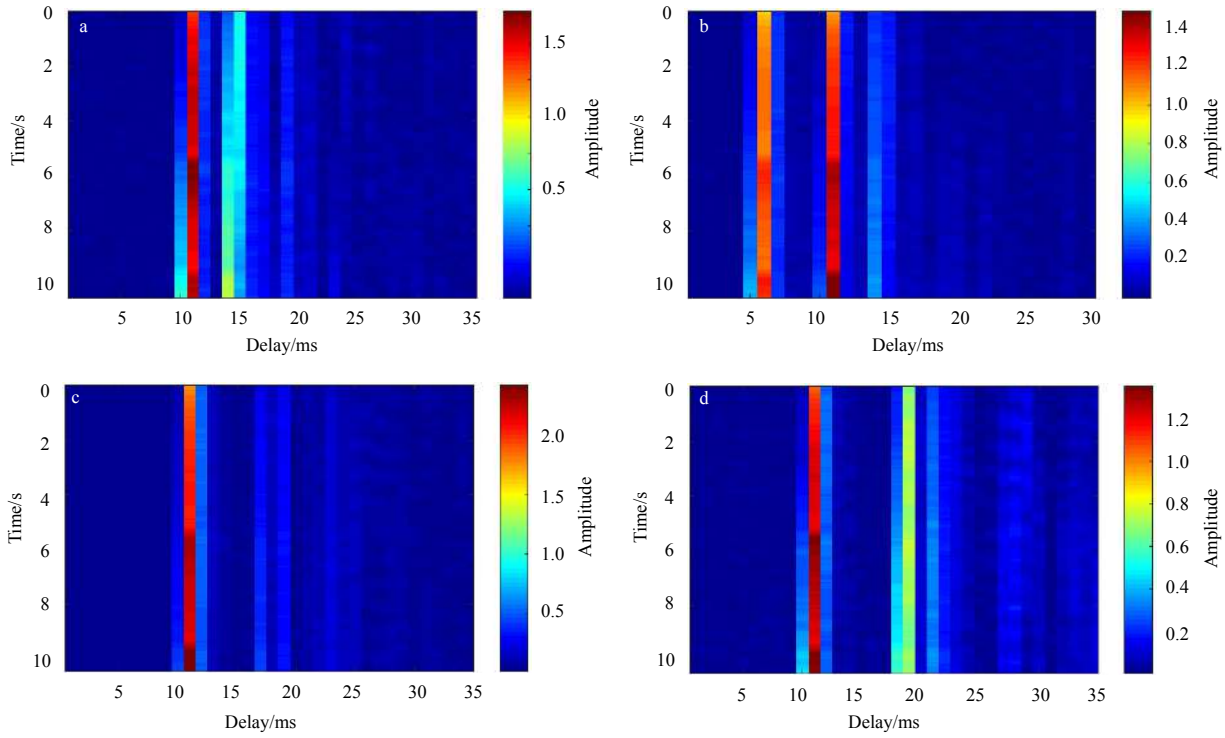

Fig. 2. CIRs at different depths at range 500 m. a. 30 m, b. 40 m, c. 50 m, and d. 60 m.

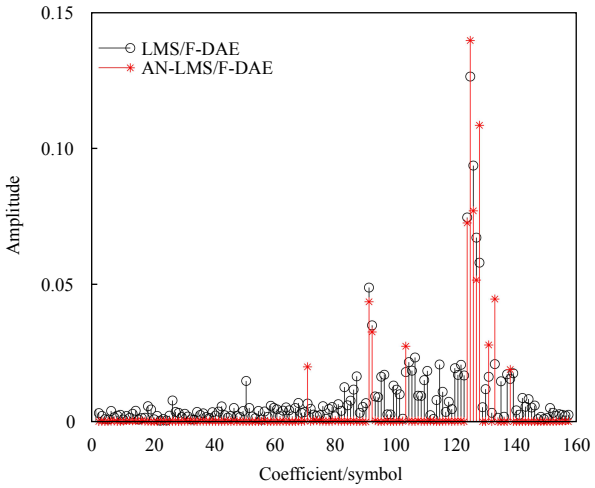

Fig. 3. Equalizer tap coefficients at range 500 m.

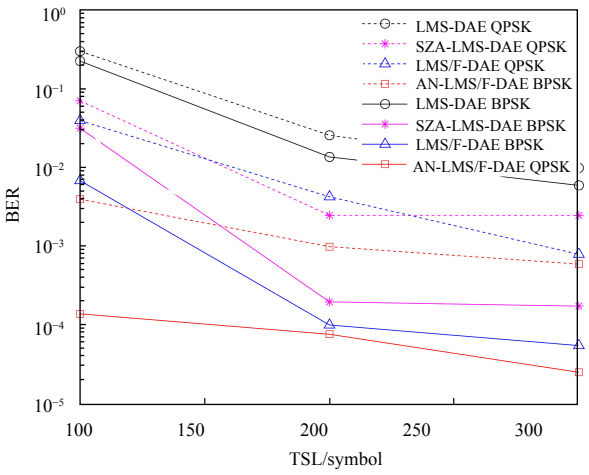

Fig. 4. BER performance under different TSLs.

The channels at range 4 km also show sparsity and they are also very stable just as shown in Fig. 2, but the structures of the channels are more complicated with much bigger multipath spread (>10 ms).

For experimental data at range 4 km, the SNR is very low. After going through a bandpass filter, the measured SNR is around 4.4 dB. The step size is set to be 0.002. In AN-LMS/F-DAE, we select $\gamma_w=3e-2, \gamma_f=5e-3, \varepsilon=1$ for BPSK modulated signal and $\gamma_w=2e-3, \gamma_f=1e-3\ \varepsilon=1.5$ for QPSK modulated signal; in SZA-LMS-DAE, $\beta=0.5, \gamma_1=3e-2, \gamma_2=5e-3$ for BPSK signal and $\beta=0.5, \gamma_1=2e-3, \gamma_2=1e-3$ for QPSK signal. The amplitude of the resulting equalizer tap is shown in Fig. 6 which also exhibits sparse feature. The structure of the equalizer in Fig. 6 is more complicated and not as sparse as that in Fig. 3.

When the communication distance is 4 km, the trend of the BERs is demonstrated in Fig. 7. The results are consistent with those at range 500 m. The LMS/F-DAE outperforms the LMS-DAE counterpart in terms of convergence speed and equalization error. Although the performance improvement of AN-LMS/F-DAE is not as obvious as that in Fig. 4, it still outperforms LMS/F-DAE and shows the best performance.

4 Conclusions

In view of the sensitivity of the LMS-DAE to the input signal and SNR, this paper proposes an LMS/F-DAE which is capable of processing complex signals for UWA communication system. Take advantage of the sparse nature of the equalizer, a variable norm constraint is added to get the AN-LMS/F-DAE. It exerts

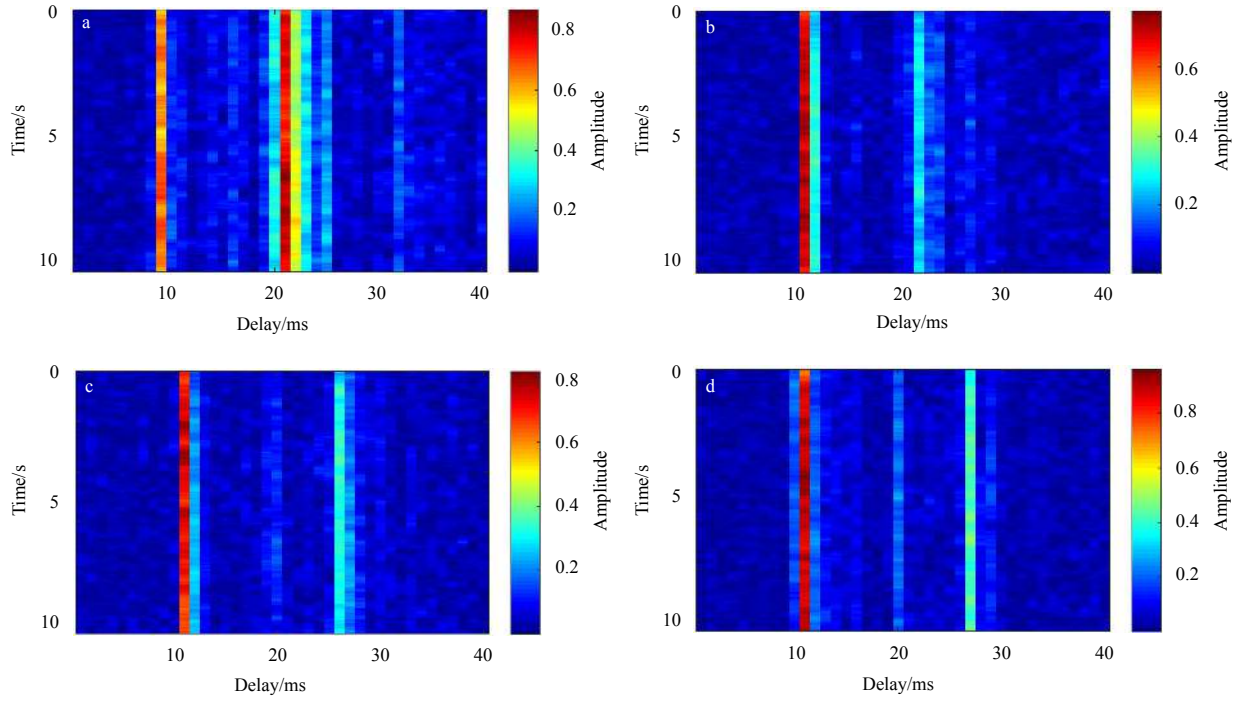

Fig. 5. CIRs at different depths at range 4 km. a. 20 m, b. 30 m, c. 50 m, and d. 60 m.

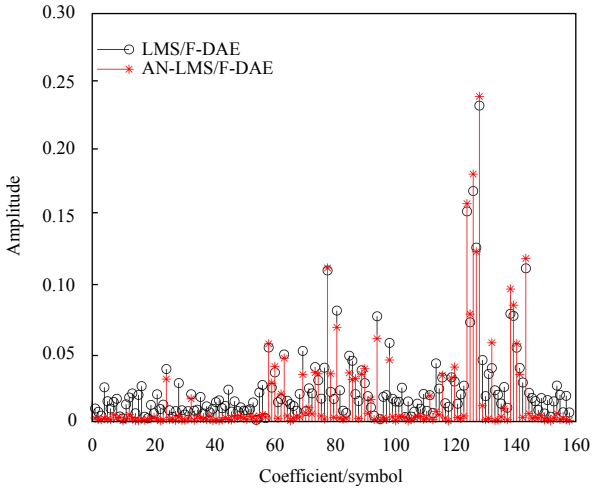

Fig. 6. Equalizer tap coefficients at range 4 km.

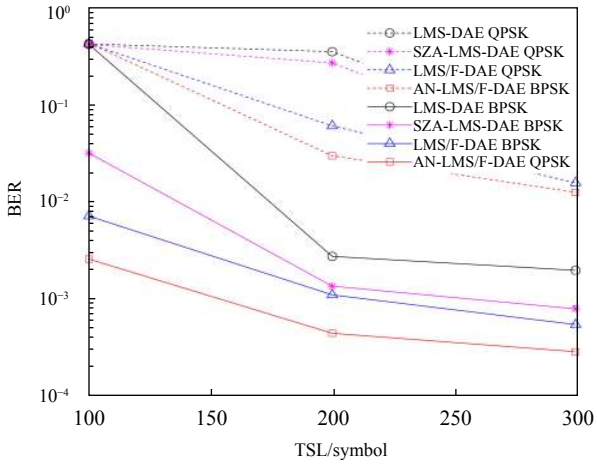

Fig. 7. BER performance under different TSLs.

constraints on small equalizer coefficients to converge quickly while exerting no constraints on large ones to ensure correct convergence. Therefore, it exhibits better performance in terms of convergence speed and equalization error. The experimental results of the 9th Chinese National Arctic Research Expedition confirm that compared with LMS/F-DAE, AN-LMS/F-DAE promotes the sparse level of the equalizer making most coefficients approach zero. Furthermore, it has better equalization performance than LMS/F-DAE.

Acknowledgements

We thank all participants of the Acoustic Communication Experiment of the 9th Chinese National Arctic Research Expedition for their assistance.

References

Berger C R, Zhou Shengli, Preisig J C, et al. 2010. Sparse channel estimation for multicarrier underwater acoustic communication: from subspace methods to compressed sensing. IEEE Transactions on Signal Processing, 58(3): 1708–1721, doi: 10.1109/TSP.2009.2038424

Brandwood D H. 1983. A complex gradient operator and its application in adaptive array theory. IEE Proceedings H Microwaves, Optics and Antennas, 130(1): 11–16, doi: 10.1049/ip-h-1.1983.0004

Chen Yilun, Gu Yuantao, Hero A O. 2009. Sparse LMS for system identification. In: 2009 IEEE International Conference on Acoustics, Speech and Signal Processing. Taipei, Taiwan: IEEE, 3125–3128

Duan Weimin, Tao Jun, Zheng Y R. 2018. Efficient adaptive turbo equalization for multiple-input-multiple-output underwater acoustic communications. IEEE Journal of Oceanic Engineer-

ing, 43(3): 792–804, doi: 10.1109/JOE.2017.2707285
Eksioglu E M. 2014. Group sparse RLS algorithms. International Journal of Adaptive Control and Signal Processing, 28(12): 1398–1412, doi: 10.1002/acs.2449
Eksioglu E M, Tanc A K. 2011. RLS algorithm with convex regularization. IEEE Signal Processing Letters, 18(8): 470–473, doi: 10.1109/LSP.2011.2159373
Falconer D, Ariyavisitakul S L, Benyamin-Seeyar A, et al. 2002. Frequency domain equalization for single-carrier broadband wireless systems. IEEE Communications Magazine, 40(4): 58–66, doi: 10.1109/35.995852
Freitag L, Koski P, Morozov A, et al. 2012. Acoustic communications and navigation under Arctic ice. In: 2012 Oceans. Hampton Roads, VA, USA: IEEE, 1–8
Guan Gui, Mehbodniya A, Adachi F. 2013a. Least mean square/fourth algorithm for adaptive sparse channel estimation. In: 2013 IEEE 24th Annual IEEE International Symposium on Personal, Indoor, and Mobile Radio Communications. London, UK: IEEE, 296–300
Guan Gui, Wei Peng, Adachi F. 2013b. Adaptive system identification using robust LMS/F algorithm. International Journal of Communication Systems, 27(11): 2956–2963
Lee Y, Cox D C. 1997. Adaptive DFE with regularization for indoor wireless data communications. In: IEEE Global Telecommunications Conference. Conference Record. Phoenix, AZ, USA: IEEE, 47–51
Li Haili, Ke Changqing, Zhu Qinghui, et al. 2019. Spatial-temporal variations in net primary productivity in the Arctic from 2003 to 2016. Acta Oceanologica Sinica, 38(8): 111–121, doi: 10.1007/s13131-018-1274-5
Li Weichang, Preisig J C. 2007. Estimation of rapidly time-varying sparse channels. IEEE Journal of Oceanic Engineering, 32(4): 927–939, doi: 10.1109/JOE.2007.906409
Liu Lu, Sun Dajun, Zhang Youwen. 2017. A family of sparse group lasso RLS algorithms with adaptive regularization parameters for adaptive decision feedback equalizer in the underwater acoustic communication system. Physical Communication, 23: 114–124, doi: 10.1016/j.phycom.2017.03.005
Mendel J M. 1991. Tutorial on higher-order statistics (spectra) in signal processing and system theory: theoretical results and some applications. Proceedings of the IEEE, 79(3): 278–305, doi: 10.1109/5.75086
Pelekanakis K, Chitre M. 2010. Comparison of sparse adaptive filters for underwater acoustic channel equalization/estimation. In: 2010 IEEE International Conference on Communication Systems. Singapore, Singapore: IEEE, 395–399
Pelekanakis K, Chitre M. 2013. New sparse adaptive algorithms based on the natural gradient and the l_0 -norm. IEEE Journal of Oceanic Engineering, 38(2): 323–332, doi: 10.1109/JOE.2012.2221811
Stojanovic M, Catipovic J, Proakis J G. 1993. Adaptive multichannel combining and equalization for underwater acoustic communications. The Journal of the Acoustical Society of America, 94(3): 1621–1631, doi: 10.1121/1.408135
Tao Jun, An Liang, Zheng Y R. 2017. Enhanced adaptive equalization for MIMO underwater acoustic communications. OCEANS 2017-Anchorage. Anchorage, AK, USA: IEEE, 1–5
Vanbleu K, Ysebaert G, Cuypers G, et al. 2006. Adaptive bit rate maximizing time-domain equalizer design for DMT-based systems. IEEE Transactions on Signal Processing, 54(2): 483–498, doi: 10.1109/TSP.2005.861901
Vlachos E, Lalos A S, Berberidis K. 2012. Stochastic gradient pursuit for adaptive equalization of sparse multipath channels. IEEE Journal on Emerging and Selected Topics in Circuits and Systems, 2(3): 413–423, doi: 10.1109/JETCAS.2012.2214631
Walach E, Widrow B. 1984. The least mean fourth (LMF) adaptive algorithm and its family. IEEE Transactions on Information Theory, 30(2): 275–283, doi: 10.1109/TIT.1984.1056886
Wang Yanshuo, Huang Fei, Fan Tingting. 2017. Spatio-temporal variations of Arctic amplification and their linkage with the Arctic oscillation. Acta Oceanologica Sinica, 36(8): 42–51, doi: 10.1007/s13131-017-1025-z
Wu Feiyun, Tong Feng. 2013. Non-uniform norm constraint LMS algorithm for sparse system identification. IEEE Communications Letters, 17(2): 385–388, doi: 10.1109/LCOMM.2013.011113.121586